Stability of Localized Patterns in Neural Fields

Konstantin Doubrovinski[1]*, J. Michael Herrmann[2]

[1]Max Planck Institute for the Physics of Complex Systems
Div. Biological Physics, Nöthnitzer Str. 38, 01187 Dresden, Germany
[2]Göttingen University, Institute for Nonlinear Dynamics
and Bernstein Center for Computational Neuroscience
Bunsenstr. 10, 37073 Göttingen, Germany

kodo7115@mpipks-dresden.mpg.de, michael@nld.ds.mpg.de

August 16, 2021

Abstract

We investigate two-dimensional neural fields as a model of the dynamics of macroscopic activations in a cortex-like neural system. While the one-dimensional case has been treated comprehensively by Amari 30 years ago, two-dimensional neural fields are much less understood. We derive conditions for the stability for the main classes of localized solutions of the neural field equation and study their behavior beyond parameter-controlled destabilization. We show that a slight modification of original model yields an equation whose stationary states are guaranteed to satisfy the original problem and numerically demonstrate that it admits localized non-circular solutions. Generically, however, only periodic spatial tessellations emerge upon destabilization of rotationally-invariant solutions.

1 Introduction

Neural fields (Amari 1977) describe the dynamics of distributions of activity on a layer of neurons. Neural fields have been suggested as models of internal representations in natural agents (Takeuchi and Amari 1979, Gross *et al.* 1998) as well as in robots (Steinhage 2000, Iossifidis and Steinhage 2001, Erlhagen and Bicho 2006). Various modalities are covered such as spatial localization, viewing direction, attentional spotlight, the dynamics of decision making, elementary behaviors, and positions of other agents in the environment. More extensive studies in theoretical neuroscience (Suder *et al.* 1999, Mayer *et al.* 2002, Bressloff 2006) concentrate on primary visual cortex, cf. (Lieke *et al.* 1989),

---

*present address: Universität des Saarlandes, Postfach 151150, 66041 Saarbrücken

superior culliculus (Schierwagen and Werner 1996), the representation of motoric primitives (Thelen *et al.* 2001, Erlhagen and Schöner 2002), and working memory in prefrontal cortex (Schutte *et al.* 2003, Camperi and Wang 1998).

Recently neural fields are experiencing attention in modeling and analysis of brain imaging data, because they are able to represent the dynamic interaction of an active medium with time-varying inputs, and because the spatial and temporal scales in the data and neural field models are starting to become comparable. Especially if information about connectivity is available from the data (Jirsa *et al.* 2002) then neural fields are of high explanatory power.

Moreover the analysis has reached a level where applications directly benefit from the theoretical progress, and at the same time, computational power became available that allows us to perform on-line simulations of two-dimensional neural fields.

Generally speaking, neural fields serve as nonparametric representations of probability densities and their dynamics may perform operations on the densities such as Bayesian computations (Herrmann *et al.* 1999). One-dimensional problems have been comprehensively studied already in the 1970s (Amari 1977, Kishimoto and Amari 1979, Takeuchi and Amari 1979). While for spatially extended, e.g. periodic patterns, the transition to the more relevant two-dimensional case is nontrivial but fairly well understood (Ermentrout and Cowan 1979, Ermentrout 1998), localized activities in dimensions larger than one have not yet been treated with the same rigor. The situation, however, does not seem to be exactly complex: a large body of numerical studies together with theoretical considerations (Laing *et al.* 2002, Laing and Troy 2003) imply a general instability of multi-bump solutions if the interactions are excitatory at small and inhibitory at large distances (see also Laing and Chow (2001) for stability analysis in one-dimensional models of spiking neurons). Further, there has been numerical evidence that single-bump solutions in two dimensions for radially symmetric interactions are essentially circular, which was exploited as an assumption in Taylor's early attack to the two-dimensional case (Taylor 1999). In ref. (Werner and Richter 2001) evidence has been provided for the existence of ring-shaped solutions which are possible for certain types of neural interactions. Along these lines one may conjecture that finite mesh-like structures of higher genus do exist as well.

The situation became more spirited only recently when in Refs. (Herrmann *et al.* 2004, Bressloff 2005, Doubrovinski 2005) the stability problem of localized activations in two-dimensional fields was eventually tackled. Although the generality which has been achieved in the one-dimensional neural fields is presently out of reach in two dimensions, a number of interesting variants of the circular activity configurations were analyzed so far.

Here we present a concise and reproducible scheme for the analysis of the stability of localized activity distributions in neural fields. We show the applicability of the scheme not only to the special case of circular solution but study also ring-shaped and bar-shaped solutions which present the complete set of known localized solutions for simple kernels (Werner and Richter 2001). In addition to the stability proofs which are based on the classical scheme (Pis-

men 1999, Bressloff 2005, Doubrovinski 2005), we are interested mainly in the behavior beyond the phase transitions towards the unstable regions. The destabilization of circular solution is known to lead to a transient elongation of the activity bubble (Bressloff 2005, Doubrovinski 2005) which ultimately causes the localized solution to split or to form meandering bands. Either case is unstable in a strict sense: the splitting into two continues toward a plane-filling hexagonal pattern while the banded patterns develop a global stripe pattern or a quasiperiodic arrangement.

The destabilization is thus fundamental since for typical Mexican-hat interaction kernels there is no nearby stable state which is approached after the bifurcation, while the spatially extended patterns are not approached in finite time (unless a general criterion for convergence is drawn into consideration). Yet the destabilization, at least in the neurobiological applications is the most interesting part of the theory. Divergences are usually very slow and may halt completely due to reasonable boundary conditions (cf. below), such that an activity-based correlational learning scheme may organize anisotropies in the connections which stabilizes the anisotropic activities as assumed in Ref. (Bressloff 2005) and exploited in (Schierwagen and Werner 1996). A theoretical account of the interaction of activity dynamics and learning was studied in (Dong and Hopfield 1992), in relation to activity effect on feature maps cf. (Mayer *et al.* 2002).

2   The neural field equation

The neural field model describes the activations of a layer of neurons when the geometry of interactions rather than the specific connectivity among the neurons is relevant. We assume positions $\mathbf{r} \in \mathbb{R}^2$ for neurons with continuous-valued activations $u(\mathbf{r}, t)$. The synaptic weights between neurons at the positions $\mathbf{r}$ and $\mathbf{r}'$ is expressed by isotropic interaction kernel $w(\mathbf{r}, \mathbf{r}') = w(|\mathbf{r} - \mathbf{r}'|)$ of Mexican-hat shape. Neurons are activated if their total input is greater than zero. We will study only equilibrium solutions without external input, and we neglect slow learning effects, so the synaptic weights are constant over time.

The activation at a position results from a weighted integration over the inputs from all other active locations in the field and a natural decay towards a resting potential denoted by h. The dynamics of the neural field is thus determined by the equation

$$\tau \frac{\partial u(\mathbf{r}, t)}{\partial t} = -u(\mathbf{r}, t) + \int_{R[u]} w(|\mathbf{r} - \mathbf{r}'|) \, d\mathbf{r}' + h, \qquad (1)$$

where $R[u] = \{x \mid u(\mathbf{r}) > 0\}$ is the excited region, i.e. a neuron receives input only from neurons within R. The boundary of $R[u]$ is assumed to be smooth. Rescaling time, τ can be set to unity without loss of generality. Equilibrium solutions are defined by

$$u(\mathbf{r}, t) = \int_{R[u]} w(|\mathbf{r} - \mathbf{r}'|) \, d\mathbf{r}' + h \qquad (2)$$

and depend on the value of the threshold parameter h and the particular form of w. Here we use a smooth kernel which is more general than the quasi-constant kernel function in Ref. (Herrmann *et al.* 2004). The kernel is constructed as a difference of Gaussian functions and is defined by four parameters K, k, M, m:

$$w = K \exp\left(-k \left\| \mathbf{r} - \mathbf{r}' \right\|^2\right) - M \exp\left(-m \left\| \mathbf{r} - \mathbf{r}' \right\|^2\right) \tag{3}$$

If non-rotationally symmetric solutions are excluded from the beginning from the consideration of Eq. 2, the situation simplifies dramatically and it can be shown (Taylor 1999) that one-bump solutions $u\left(\left\|\mathbf{r}\right\|\right)$ of certain radii are stationary states of the dynamics (1). Analogously, a ring-shaped solution (Werner and Richter 2001) or a stripe-like solution, i.e. a degenerate ring of infinite radius, can occur. However, when considering an arbitrarily small perturbation of the solution, the symmetry might be broken and new phenomena can appear, as will be studied in the following.

3   Stability

It has previously been shown that (1) admits rotationally invariant stationary solutions with disc-shaped activated region (one-bump solutions). Generically, these arise in the course of a "blue sky bifurcation" (Strogatz, 1994): no solution is present in the subcritical parameter region whereas two solution branches bifurcate as control parameter exceeds the critical value. The two solutions are rotationally invariant one-bumps. Stability analysis of these states with respect to rotationally invariant perturbation is essentially equivalent to stability analysis of one-bump solution of the one-dimensional model. It reveals that the unstable branch generically corresponds to the bump of smaller radius. Upon destabilization the region of activation expands as the solution approaches the stable branch, corresponding to the circular bump of larger radius (See Fig. 1).
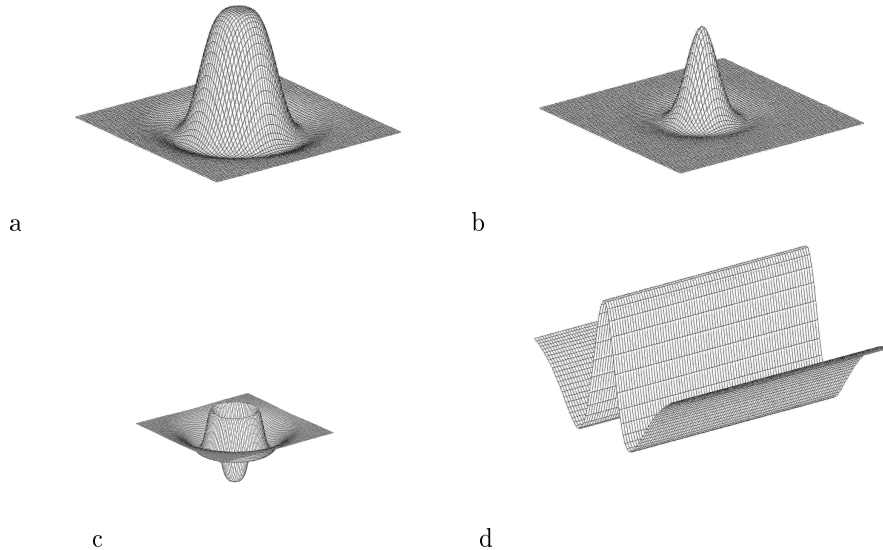
Figure 1: (a) Stable one-bump solution of the neural field equation. Parameters are $K = 2.5$, $k = 5$, $M = 0.5$, $m = 0.5$, $h = -0.281$ (b) Unstable one-bump solution for the parameter values $K = 2.5$, $k = 5$, $M = 0.5$, $m = 0.5$, $h = -0.294$ (c) Annular solution with the parameters $K = 2.5$, $k = 5$, $M = 0.5$, $m = 0.5$, $h = -0.115$ (d) A part of a stable stripe-like solution. Parameters are the same as in (c). At the same parameters also an unstable solution exists (not shown).

Seeking a stationary solution $\overline{u}$ of the two-dimensional model (1) assuming rotational invariance of the field (i.e. $\overline{u}(\mathbf{r}) \equiv \overline{u}(r)$ with $r = \|\mathbf{r}\|$) leads to a problem, essentially equivalent to that of finding stationary states in the one-dimensional model (see Appendix). Two types of solutions besides the circular one-bumps are readily constructed: solutions with annular activated regions and solutions with stripe-shaped region of activation (see Fig. 1). The possibility of existence of the former has been pointed out previously, whilst the latter can be seen as degenerate annuli of infinite inner radius.

We now turn to the analysis of the stability properties of the above-mentioned stationary states. Consider the one-bump solution with disc-shaped activated region (i.e. $u(r) > 0$ iff $r < R$). Consider dynamics of a small perturbation $\epsilon\eta$, i.e.

$$u(\mathbf{r}, t) = \overline{u}(\|\mathbf{r}\|) + \epsilon\eta(r, t) \tag{4}$$

Inserting into (1) and keeping terms of order at most 1 in ϵ one finds that to linear order the dynamics of the perturbation obeys

$$\frac{\partial \eta(\mathbf{r}, t)}{\partial t} = -\eta(\mathbf{r}, t) + \int_{\mathbb{R}^2} w(\|\mathbf{r} - \mathbf{r}'\|)\, \delta(\overline{u}(\mathbf{r}'))\, \eta(\mathbf{r}', t)\, d\mathbf{r}' \tag{5}$$

5

where $\delta\left(\overline{u}\left(\mathbf{r}'\right)\right)$ is Dirac delta function (see Appendix). Substituting an Ansatz of the form $\eta\left(\mathbf{r}, t\right) = \exp\left(\lambda t\right)\xi\left(\mathbf{r}\right)$ one arrives at an eigenvalue problem which in polar coordinates becomes (see Appendix)

$$\lambda\xi\left(r, \theta\right) = -\xi\left(r, \theta\right) + \Gamma\int_0^{2\pi} g\left(\theta - \theta'\right)\xi\left(r, \theta'\right) d\theta' \tag{6}$$

Here g is a 2π periodic function depending on kernel $w\left(\|\mathbf{r} - \mathbf{r}'\|\right)$ and Γ is a constant given by

$$\Gamma = R\left|\frac{\partial\overline{u}\left(r\right)}{\partial r}\right|_{r=R}\Bigg|^{-1} \tag{7}$$

i.e. the ratio of the radius of activated region R to the absolute value of the slope of the radial profile of the stationary solution at $r = R$. Clearly, explicit evaluation of Γ requires calculating the stationary solution which is implicitly given by (2) in terms of a double integral. Equation (6) is known as Fredholm's integral equation of the second kind. The integral operator in the right-hand side of (6) is compact, bounded and self-adjoint implying that every spectral value is an eigenvalue, all eigenvalues are real, each eigenspace is finite-dimensional and zero is the only possible accumulation point of eigenvalues (Kreyszig, 1978). Solving (6) we obtain eigenvalues and eigenfunctions which in polar coordinates read (see Appendix)

$$\lambda_n = -1 + \Gamma\int_0^{2\pi} g\left(\theta\right)\cos\left(n\theta\right) d\theta$$
$$\xi_n = \int_0^{2\pi} w\left(r, \theta, R, \theta'\right)\cos\left(n\theta'\right) d\theta' \tag{8}$$

where R is the radius of the circular activated region. The nth eigenfunction is $2\pi n$-periodic in θ, implying that it is D_n-symmetric (symmetry with respect to rotation by $2\pi/n$ around the origin and with respect to reflections on the n respective symmetry planes; the shape in Fig. 5a, e.g., is D_4-symmetric) and corresponds to a multi-periodic deformation of a circle. Eigenvalue spectra for one-bump solutions are given in Fig. 2. Certain features of these are readily interpretable. E.g. we see that for the bump of smaller radius the eigenvalue λ_0, corresponding to rotationally invariant deformation, is positive implying instability with respect to perturbations in radius of the bump. The spectrum, corresponding to the larger bump, however, is non-positive, implying stability with respect to arbitrary perturbation in agreement with earlier results. Also, the eigenvalue λ_1, that corresponds to a 2π-periodic deformation (or, equivalently, to a translation of the bump) vanishes, reflecting the translational invariance of (1). Exploiting this observation, it appears possible to re-express Γ in (7) more explicitly as $\Gamma = 1/\int_0^{2\pi} g\left(\theta\right)\cos\left(\theta\right) d\theta$, whereby the expressions for the other eigenvalues simplifies to

$$\lambda_n = -1 + \frac{\int_0^{2\pi} g\left(\theta\right)\cos\left(n\theta\right) d\theta}{\int_0^{2\pi} g\left(\theta\right)\cos\left(\theta\right) d\theta} \tag{9}$$
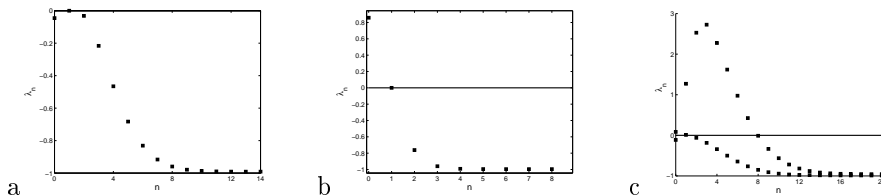
Figure 2: Spectra of corresponding to solutions in Fig. 1 a, b, and c, respectively. The positivity of the zeroth mode in (b) indicates the instability of this solution with respect to circular perturbations. The solution (a) is stable, with a marginal instability with respect lateral shift as visible from the vanishing first eigenvalue. The instability of the annulus solution in (c) shows a characteristic scale which causes the solution to split into three single bumps.

Note that contrary to (8), Eq. 9 does not contain explicitly the stationary solution $\overline{u}$, which allows us to calculate the nth eigenvalue as a function of the radius of activated region without evaluating double integrals in the implicit expression for $\overline{u}$. Only integrals over one-dimensional manifolds appear in (9), greatly simplifying the calculation of the spectrum. Apart from theoretical considerations, this is of importance for technical applications since the knowledge of stability properties of solutions of (1) could affect their use for representing probability distributions e.g. in implementations of autonomous robot memory.
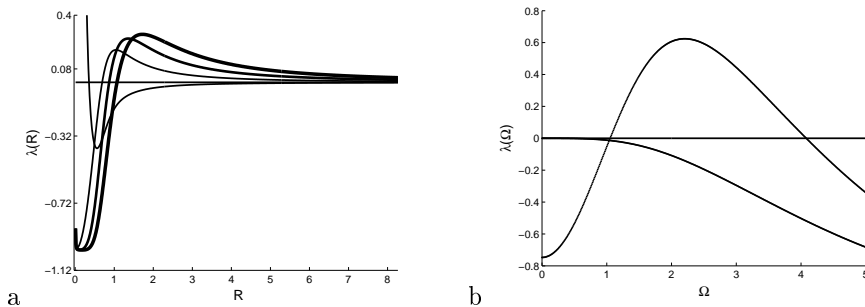

Figure 3: (a) Four eigenvalues versus bump radius R. The curve which represents λ_0 described the stability with respect to perturbations in bump radius. The others are (from left to right) λ_2 (reflection-invariant deformation), λ_3 (D_3-invariant eigenmode) and λ_4 (D_4-invariant eigenmode). λ_1 is identically zero reflecting the metastability of the solutions w.r.t. lateral shifts. Parameters are: $K = 1.5$, $k = 5$, $M = 0.5$, $m = 1.5$ (b) Spectrum determining stability of stripe-shaped solutions shown in Fig. 1(d). Only the information for the stable solution if given here. This solution looses stability for a band of values of Ω.

Previous work (Werner-Richter 2001) conjectured the bifurcation branch cor-

responding to the stable one-bump to remain stable for all values of control parameter. Using (9) this is readily proved false: higher and higher frequency eigenmodes progressively turn unstable as the radius of the stationary solution is increased (see Fig. 3).

Strictly speaking, the assertion that linear stability analysis as outlined above correctly determines stability properties of stationary solutions relies on additional assumptions on operators appearing in the right-hand side of (1) (Schaefer and Golubitsky 1988). For infinitely-dimensional non-smooth fields these generically need not hold. In order to check whether stability analysis is indeed adequate, correctly determining stability properties of the stationary solutions, we performed a number of numerical simulations. Fig. (4) depicts a simulation of unstable one-bump whose corresponding stability spectrum reveals that the maximal (positive) eigenvalue is that of the D_2-symmetric eigenmode. As the time elapses, initially circular activated region keeps deforming, forming blob-like protrusions. These subsequently bud off from the middle-bump. The newly-formed activated domains keep splitting, progressively tiling the plane in a hexagonal pattern. We would like to stress that the pattern which is formed immediately after destabilization of the stationary state is D_2-symmetric as would be expected from the properties of the eigenvalue spectrum. That is, stability properties of the stationary solutions as well as qualitative aspects of the pattern, forming upon destabilization of the steady state, are correctly predicted from the above-mentioned linear stability analysis.

Figure 4: (Upper panel) Time evolution of an unstable bump, undergoing stability loss at a D_2-eigenmode. Parameters are: $K = 1.5$, $k = 5$, $M = 0.5$, $m = 1.5$, $h = -1.46 \cdot 10^{-2}$. (Lower panel) Time evolution of an unstable bump, undergoing stability loss at a D_3 invariant eigenmode. Parameters: $K = 1.5$, $k = 5$, $M = 0.5$, $m = 1.5$, $h = -4.43 \cdot 10^{-3}$.

Symmetry breaking accompanying destabilization of a stationary bump was examined for a broad range of parameters (e.g. parameters which yielded solutions with maximal eigenvalue of the respective spectrum corresponding to D_3-, D_4- and D_8-symmetric perturbations, see Fig. 4). In all of the cases, the course of the symmetry breaking was appropriately determined by linear stability.

Stability analysis of annular solutions proceeds along the same lines as that

of one-bumps (see Appendix). The essential difference is that instead of a singe equation (6), a system of two equations results, meaning that to every non-negative whole number corresponds a pair of real eigenvalues. (In general, to every boundary of an activated domain there corresponds an equation in the corresponding eigenvalue problem). We find that in the case of annular solution shown in Fig. 1d the largest eigenvalue corresponds to a D_3-symmetric perturbation. Simulations demonstrate that initially rotationally invariant annulus splits into three adjacent blobs which gradually drift apart (not shown). The symmetry of the resulting state is the same as that of the largest eigenvalue. Again, stability of the stationary solution as well as qualitative aspects of the emerging pattern are readily predicted from the analytically computed spectrum.

Finally, let us consider the stripe-shaped solutions. Their stability is governed by an eigenvalue problem, similar to that governing stability of the annuli. However, the corresponding linear operator is no longer compact (this is a consequence of activated region being unbounded) and the spectrum needs no longer remain discrete. Actually, in this case the spectrum is continuous: to every real corresponds a pair of (real) eigenvalues. Fig. 3b shows results of linear stability analysis of the stripe solution, depicted in Figure 1d. In the corresponding simulation the stripe is seen to split into a row of separate bumps – a "chain-of-pearls" configuration. The inter-bump separation is the same as the wave-length of the eigenmode, corresponding to the largest eigenvalue. Again, stability and semi-quantitative properties of patterns resulting from the stationary state destabilization are readily predicted from the respective eigenvalue spectrum.

In summary, preceding section describes all of the stationary non-homogeneous solutions of the two-dimensional Amari equation known up to date and exhaustively examines their stability properties. Quite strikingly, stability analysis of the non-homogeneous steady state is possible since the eigenvalue problem (8) is effectively one-dimensional although a two-dimensional system is being considered.
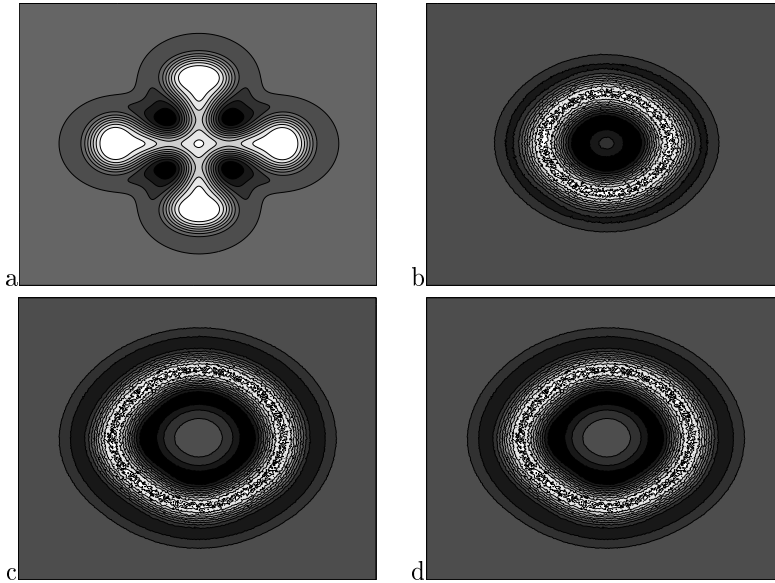
Figure 5: Dynamics of the modified field with and without noise. (a) In the absence of noise an unstable bump develops four identical protrusions subsequently splitting into four separate blobs. (b) In presence of noise a ring-shaped region of activation is initially annular, but (c and d) develops gradually into an irregularly meandering profile. Parameters are $k = 5$, $m = 1.6$, $K = 1.5$, $M = 0.45$, $h = -0.0505$, $p = -6.25 \cdot 10^{-4}$.

4 Modified equation

A long-standing question regarding Amari-model is existence of non-rotationally invariant stationary solutions with bounded and connected region of activation. Such states are likely to bifurcate from circular solutions upon destabilization at a non-rotationally invariant eigenvalue. In fact, stability loss of one branch is always accompanied by emergence of another in its vicinity provided that the mappings defining the dynamical system under consideration are sufficiently smooth (Crandall and Rabinowitz 1971). However, in the above simulations exclusively periodic patterns resulted upon destabilization of circular solutions.

In order to address existence of non-rotationally invariant solutions of (1) with bounded and connected activated region we shall modify the original Amari-model (1) so as to obtain a related ("modified") equation fulfilling the following three conditions.

1. Stationary solutions of the modified equations should be solutions of the unmodified equation (2).

2. The modified equation should not admit solutions with unbounded activated region.

10

3. Stability of a solution of Eq. (2) should remain unaltered by the modification.

According to condition 3 rotationally invariant stationary solutions behave like those of the unmodified Amari-model, admitting symmetry breaking at a non-rotationally invariant eigenvalue. However, the symmetry breaking cannot result in a spatially extended periodic pattern according to condition 2. Consequently, a non-rotationally invariant localized state is likely to emerge. It will be a solution of the original (unmodified) Amari model with desired properties, provided that its region of activation remains connected in the course of destabilization. Note, however, that conditions 1-3 do not suffice to ensure that the activated domain will not start splitting into separate disconnected region upon symmetry breaking.

We now turn to the construction of a modification of (1) satisfying the above-mentioned conditions 1-3. Consider some circular one-bump solution $\overline{u}_h$ of (1) with resting potential h and the area of activated region $A[\overline{u}_h]$. Let us modify (1) according to

$$\partial_t u = -u\left(\mathbf{r}, t\right) + \int_{R[u]} \left[w\left(|\mathbf{r} - \mathbf{r}'|\right) + q\right] d\mathbf{r}' - qA[\overline{u}_h] + h' \qquad (10)$$

where q is any real number. Suppose that $\overline{u}$ is a stationary solution of (10) for a certain q. Substituting $\overline{u}$ into (10) one obtains with the area of $R[\overline{u}]$ being denoted by $A[\overline{u}]$:

$$0 = -\overline{u}\left(\mathbf{r}, t\right) + \int_{R[\overline{u}]} \left[w\left(|\mathbf{r} - \mathbf{r}'|\right) + q\right] d\mathbf{r}' - qA[\overline{u}_h] + h' =$$
$$= -\overline{u}\left(\mathbf{r}, t\right) + \int_{R[\overline{u}]} w\left(|\mathbf{r} - \mathbf{r}'|\right) d\mathbf{r}' + qA[\overline{u}] - qA[\overline{u}_h] + h' \qquad (11)$$

implying that $\overline{u}$ is a solution of (2) with the resting potential h replaced by $h' - qA[\overline{u}_h] + qA[\overline{u}]$. Consequently, condition 1 is satisfied. Note that the circular one-bump solution $\overline{u}_h$ of the original problem (2) which was used when constructing (10) solves the modified problem (10) with $h' = h$ and any q.

Eq. (10) does not admit stationary solutions with unbounded region of activation. Indeed, assuming that such a solution $\hat{u}$ exists, substituting $\hat{u}$ into (10) we were to conclude that the integral term of the right-hand-side of (10) is infinite which forms a contradiction. Therefore condition 2 above is satisfied.

Finally, we show that the modification (10) preserves stability properties of the stationary solution $\overline{u}_h$ (which is a stationary solution of both the modified and the unmodified problems (1) and (10) respectively by construction). Recall that in deriving equation (8) we did not make use of any particular assumptions on the form of the integral kernel $w\left(|\mathbf{r} - \mathbf{r}'|\right)$. Consequently, this expression for the eigenvalue spectrum is equally valid for the modified problem as well as for the unmodified one. Note, however, that when deriving stability spectrum in the case of the modified problem (10) we shall exchange $g\left(\theta - \theta'\right)$ by $g\left(\theta - \theta'\right) + qA[\overline{u}_h]$ (see derivations in the Appendix).

Using $\int_0^{2\pi} qA[\overline{u}_h]\cos{(n\theta)}\,d\theta = qA[\overline{u}_h]\int_0^{2\pi}\cos{(n\theta)}\,d\theta = qA[\overline{u}_h]2\pi\delta_{n0}$ it now follows from (8) that all eigenvalues of the stability spectrum of $\overline{u}_h$ (except for λ_0 corresponding to perturbations of the radius of the bump) remain unaltered by the modification. Consequently, if $\overline{u}_h$ is unstable with respect to some non rotationally-invariant perturbation in the original problem (1), it is unstable with respect to such a perturbation in the modified problem (10), whereby condition 3 holds.

The above arguments imply that a rotationally invariant solution $\overline{u}_h$ of Eq. (1) that is unstable at a non-circular eigenmode solves also the modified equation (10) and is unstable with respect to the same eigenmode of the dynamics (10). Furthermore, contrary to the case of (1), the dynamics of (10) can never result in a periodic pattern with unbounded activated region if $q < 0$.

As stated above, conditions $1-3$ do not suffice to guarantee that the activated region will remain connected as $\overline{u}_h$ follows the dynamics (10). Nevertheless, by tuning the parameter q in (10) one is able to trap the dynamics in the vicinity of instability in a state with connected activated region.
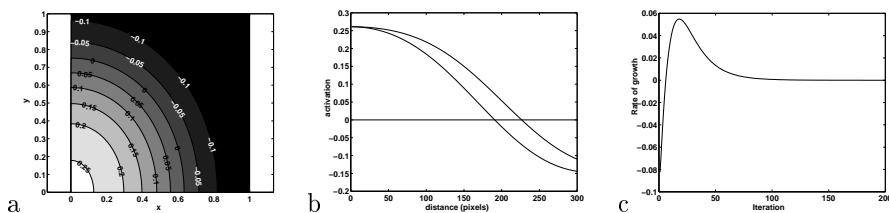

Figure 6: (a) Contour plot of the D_2-symmetric solution superimposed with its level-curves. The zeroes level-curve (corresponding to $u = 0$) delimits the activated region. The symmetries of the equation and initial condition allow to restrict the simulation to one quarter of the domain. The resulting blob is roughly ellipse-shaped with the vertical semi-axis being longer than the horizontal one. (b) Cross-section through the profile of the stationary solution along the coordinate axes. (c) Rate of growth of the solution versus iteration step calculated as maximal deviation between two subsequent time steps. Parameters are $K = 1.5$, $k = 5$, $M = 0.5$, $m = 1.5$, $h = 1.50$, $q = 0.02850$.

Assume that for $q = 0$ the dynamics in vicinity of the bifurcation tends to increase the area of the activated region. Note that q could be understood as a Lagrange multiplier, which ensures the constancy of the area for one special value, which we certainly exclude. Suppose now that q is chosen to be negative. The additional term in the integrand of (10) will tend to counterbalance the area increase. We can now choose q such that two effects counterbalance and a non-rotationally invariant steady state with bounded and connected region of activation will result. The calculation of effective values of q requires the consideration of higher orders of the dynamics which can be expressed by a Ginzburg-Landau equation, cf. Doubrovinski (2005). Here, we will instead take resort to numerical simulations. These confirm the emergence of non-rotationally invari-

ant steady states with bounded and connected region of activation. For example, Fig. 6 shows the destabilization of a circular one-bump which is unstable at a D_2-symmetric eigenmode, developing into a non-rotationally invariant steady state with ellipse-shaped activated region. Only one quarter of the domain was simulated (the field in the other three quadrants is determined by that on the simulated quadrant due to Euclidean symmetry of dynamic equations and D_2-symmetry of initial conditions) on a grid of 300×300 pixels in order to increase the accuracy. Symmetries corresponding to higher eigenvalues are irrelevant because the eigenvalues λ_n are stable for $n \geq 3$ for the given parameters. The length difference of the half-axes of the activated domain of the resulting D_2-symmetric stationary state was much larger than the spatial discretization step (some 30 pixels) allowing to conclude that that the stationary solution obtained is not a discretization artifact.

Another example is given in Fig. 7 showing the dynamics in the vicinity of stability loss at a D_3-symmetric eigenmode. Initially the field is D_3-symmetric. We see that initially a D_3-symmetric state with connected activated region does indeed result. The system dwells in this state during considerable time, breaking D_3-symmetry due to small numerical perturbations (in absence of perturbations D_3-symmetry must be preserved by the dynamics (10) due to invariance under Euclidean transformations). Supposedly, the emerging D_3-symmetric state is stable when the dynamical system is confined to the subspace of D_3-symmetric functions. The final peak in Fig. 7e, however, indicates an instability with respect to a D_2-symmetric perturbation.
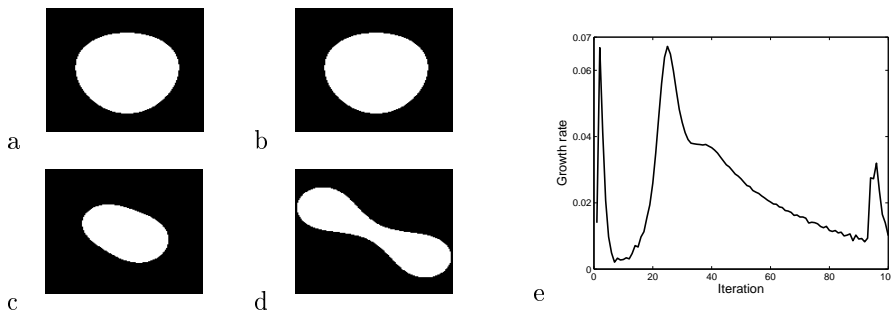

Figure 7: (a)-(d): Time evolution of activated region. (e) Rate of growth of the solution versus iteration step calculated as maximal deviation between two subsequent time steps. The initial deep "valley" corresponds to the shape of activated region shown in panel (b). Parameters are: $K = 1.5$, $k = 5$, $M = 0.5$, $m = 1.5$, $h = -0.0260$, $q = 0.0125$.

In conclusion we would like to stress that the particular choice of modification according to (10) is very restrictive. In fact, many other equations whose stationary states satisfy (1) and do not admit solutions with unbounded regions of activation are readily constructed along the same lines. For instance $\partial_t u = -u + \int_{R[u]} w\left(|\mathbf{r} - \mathbf{r}'|\right) d\mathbf{r}' - \int_{R[u]} |\mathbf{r} - \mathbf{r}'| \, d\mathbf{r}' d\mathbf{r} + h$ can be shown to have

13

these properties, arguing essentially as when proving that conditions 1 and 2 above are satisfied by stationary states of (10). We believe that further investigation of such modifications will provide insights into the properties of unstable solutions of Amari-equation.

5 The time course of symmetry breaking

Bifurcation theory describes the time course to critical behavior in low-dimensional systems. Under certain conditions the parametric destabilization of an activity distribution does not lead to a nearby stable state, but initiates a cascade of symmetry breaking events which eventually approaches a new distant stable configuration. It has been a motivation for the present study to demonstrate the complex evolution of the state of the field after the loss of stability. It is these configurations that bear the greatest computational potentials.

For the Amari equation with a simple kernel only the existence of rotationally invariant bumps has been proven. This work demonstrates existence of two other non-periodic stationary states: stripe-shaped and annular solutions. Stability analysis of these would be expected to be very involved. Surprisingly, the special form of the Amari equation makes this stability problem amenable to analytical treatment. The total synaptic input to a given neuron is only dependent on the shape of the boundary of the activated domain, making the eigenvalue problem effectively one-dimensional, thereby allowing for fairly straight-forward calculation of the spectrum for each of these cases.

Strictly speaking, spectral properties of the linearized operator do not guarantee the stability of the stationary state unless additional assumptions are satisfied. However, our extensive numerical investigation shows that stability is indeed correctly predicted by eigenvalue analysis. Furthermore, the spectrum allows to predict certain semiquantitative features of solutions approached after the onset of instability.

Our numerical experiments showed that exclusively spatially extended solutions (i.e. those with unbounded activated domain) appeared in the unstable parameter region. Yet, a slight modification of the interaction kernel, introducing long-range interactions circumvents this, yielding non-rotationally invariant stationary states with bounded and connected region of activation which at the same time are stationary states of the original unmodified equation. This settles a longstanding question regarding existence of solutions of this type. This bears also relevancy for biological systems. Assuming a certain degree of shift-twist symmetry the existence of elongated blobs suggests mechanisms for the emergence of orientation selectivity in neurons of the primary visual cortex. Although the degree of asymmetry of non-rotationally invariant solutions was moderate, these effects could in principle be enhanced by (Hebbian) learning which we disregarded in our treatment.

A Appendix

A.1 Circular one-bump solution

Consider the development of a small perturbation $\varepsilon\eta$ of a stationary rotationally-invariant one-bump $\bar{u}$. Substituting into the Amari equation and linearizing in ε we have

$$\frac{\partial\eta\left(\mathbf{x},t\right)}{\partial t} = -\eta\left(\mathbf{x},t\right) + \int_{\mathbb{R}^2} w\left(\left|\mathbf{x}-\mathbf{x}'\right|\right)\delta\left(\bar{u}\left(\mathbf{x}'\right)\right)\eta\left(\mathbf{x}',t\right)d\mathbf{x}'. \tag{12}$$

In polar coordinates we write (somewhat informally) $w\left(\left|\mathbf{x}-\mathbf{x}'\right|\right) = w\left(r,\theta,r',\theta'\right)$, and use the rotational invariance of $\bar{u}$, such that

$$\frac{\partial\eta\left(r,\theta,t\right)}{\partial t} = -\eta\left(r,\theta\right) + \int_0^{2\pi}\int_0^{\infty} r'w\left(r,\theta,r',\theta'\right)\delta\left(\bar{u}\left(r'\right)\right)\eta\left(r',\theta'\right)dr'd\theta' \tag{13}$$

Recall that

$$\delta\left(f\left(x\right)\right) = \sum_{x_i}\frac{\delta\left(x-x_i\right)}{\left|\frac{df\left(x_i\right)}{dx}\right|}, \tag{14}$$

where the sum is over the roots of f, provided that f is differentiable at the corresponding points. Using (14), (2) simplifies to

$$\frac{\partial\eta\left(r,\theta\right)}{\partial t} = -\eta\left(r,t\right) + \int_0^{2\pi} Rw\left(r,\theta,R,\theta'\right)\frac{1}{\left|\frac{\partial\bar{u}(R)}{\partial r}\right|}\eta\left(R,\theta'\right)d\theta', \tag{15}$$

where R is the radius of the (circular) region of activation of $\bar{u}$. Substituting $\eta = e^{\lambda t}\xi\left(r,\theta\right)$ we arrive at the following eigenvalue problem.

$$\lambda\xi\left(r,\theta\right) = -\xi\left(r,\theta\right) + \Gamma\int_0^{2\pi} w\left(r,\theta,R,\theta'\right)\xi\left(R,\theta'\right)d\theta', \tag{16}$$

where $\Gamma \equiv R/\left|\left(\partial\bar{u}\left(R\right)/\partial r\right)\right|$. By restriction of both sides to $r = R$, the eigenvalue problem (16) is solved by

$$\xi_n\left(R,\theta\right) = \cos n\theta$$
$$\lambda_n = -1 + \Gamma\int_0^{2\pi} w\left(R,\theta,R,0\right)\cos\left(n\theta\right)d\theta, \tag{17}$$

where n are nonnegative integers. The last equation can be verified by noting that $w\left(R,\theta,R,\theta'\right)$ is a function of $\left(\theta-\theta'\right)$ alone and Fourier-expanding the integrand of (16).

The r-dependence of the eigenfunctions can be derived from (17) by exploiting the special form of the eigenvalue problem (16).

$$\xi_n\left(r,\theta\right) = \int_0^{2\pi} w\left(r,\theta,R,\theta'\right)\cos\left(n\theta'\right)d\theta' \tag{18}$$

Shift invariance allows us to conclude that $\lambda_1 = 0$. Thus, Γ is obtained more explicitly from Eq. 17.

$$\Gamma = \frac{1}{\int_0^{2\pi} w\left(R, \theta, R, 0\right) \cos\left(\theta\right) d\theta} \tag{19}$$

Now the eigenvalues can be calculated without evaluating the slope of the stationary solution $\bar{u}$:

$$\lambda_n = -1 + \frac{\int_0^{2\pi} w\left(R, \theta, R, 0\right) \cos\left(n\theta\right) d\theta}{\int_0^{2\pi} w\left(R, \theta, R, 0\right) \cos\left(\theta\right) d\theta} \tag{20}$$

Eq. (20) is particularly convenient for examining stability properties of circular one-bump solutions.

A.2   Annular solutions

The existence of solutions with annular region of activation was suggested already in (Amari 1977). Denoting the inner radius by R_1 and the outer radius by R_2, (15) is immediately rewritten

$$\begin{aligned}
\frac{\partial \eta\left(r, \theta\right)}{\partial t} &= -\eta\left(r, \theta\right) + \Gamma_1 \int_0^{2\pi} w\left(r, \theta, R_1, \theta'\right) \eta\left(R_1, \theta'\right) d\theta' \\
&\quad + \Gamma_2 \int_0^{2\pi} w\left(r, \theta, R_2, \theta'\right) \eta\left(R_2, \theta'\right) d\theta',
\end{aligned} \tag{21}$$

where $\Gamma_1 = R_1 / \left|\partial \bar{u}\left(R_1\right) / \partial r\right|$, $\Gamma_2 = R_2 / \left|\partial \bar{u}\left(R_2\right) / \partial r\right|$. Analogously to the derivation of (16), we set $\eta = e^{\lambda t} \xi\left(r, \theta\right)$ and restrict both sides to R_1 and R_2.

$$\lambda \xi_1 = -\xi_1 + \Gamma_1 \int_0^{2\pi} w\left(R_1, \theta, R_1, \theta'\right) \xi_1' \theta' + \Gamma_2 \int_0^{2\pi} w\left(R_1, \theta, R_2, \theta'\right) \xi_2' d\theta'$$

$$\lambda \xi_2 = -\xi_2 + \Gamma_1 \int_0^{2\pi} w\left(R_2, \theta, R_1, \theta'\right) \xi_1' d\theta' + \Gamma_2 \int_0^{2\pi} w\left(R_2, \theta, R_2, \theta'\right) \xi_2' d\theta' \tag{22}$$

where $\xi_i = \xi\left(R_i, \theta\right)$ and $\xi_i' = \xi_i\left(\theta'\right)$, $i \in \{1, 2\}$. It is natural to seek the eigenfunctions of the form $[\xi_1, \xi_2] = \mathbf{v} \cos\left(n\theta\right)$, where $\mathbf{v}$ is some two-dimensional vector. Using this substitution it turns out that the eigenvalues of (22) are the same as those of the matrices

$$\begin{bmatrix} -1 + \Gamma_1 \int_0^{2\pi} w_{11} \cos n\theta d\theta & \Gamma_2 \int_0^{2\pi} w_{12} \cos n\theta d\theta \\ \Gamma_1 \int_0^{2\pi} w_{12} \cos n\theta d\theta & -1 + \Gamma_2 \int_0^{2\pi} w_{22} \cos n\theta \end{bmatrix} \tag{23}$$

such that Eq. 23 allows us to construct the spectrum of (22).

A.3   Stripe-shaped solutions

Stripe-shaped solutions can be constructed by assuming the region of activation of the form $R\left[\bar{u}\right] = \{(x, y) \mid 0 \le x \le L\}$ and can be seen as degenerate annuli

with infinite inner radius, considered in the previous section. Interestingly, in this case it appears possible to give an explicit expression for the stationary one-bump solution in terms of the model parameters:

$$\bar{u}\left(x,y\right) = \tfrac{\pi}{2km}(Km\;\mathrm{erf}\left(\sqrt{k}x\right) - kM\;\mathrm{erf}\left(\sqrt{m}x\right) - $$

$$-Km\;\mathrm{erf}\left(-\sqrt{k}L + \sqrt{k}x\right) + Mk\;\mathrm{erf}\left(-\sqrt{m}L + \sqrt{m}x\right)) - h \qquad (24)$$

The counterpart of (21) now reads

$$\frac{\partial \eta}{\partial t} = -\eta + \int_{\mathbb{R}^2} w\left(|\mathbf{x} - \mathbf{x}'|\right)\delta\left(\bar{u}\left(\mathbf{x}'\right)\right)\eta\left(d\mathbf{x}'\right)$$

$$= -\eta + \int_{-\infty}^{\infty} w\left(x,y,0,y'\right)\frac{1}{\left|\frac{\partial \bar{u}(0)}{\partial x}\right|}\eta\left(0,y'\right)dy' \qquad (25)$$

$$+ \int_{-\infty}^{\infty} w\left(x,y,L,y'\right)\frac{1}{\left|\frac{\partial \bar{u}(L)}{\partial x}\right|}\eta\left(L,y'\right)dy', \qquad (26)$$

where (x,y) and (x',y') are Cartesian coordinates of $\mathbf{x}$ and $\mathbf{x}'$ respectively. As in the former cases, substituting $\eta\left(x,y,t\right) = e^{\lambda t}\xi\left(x,y\right)$ and restricting to 0 or to L we find

$$\lambda\xi_1 = -\xi_1 + \Gamma_1\int_{-\infty}^{\infty} w\left(0,0,0,y'\right)\xi_1'dy' + \Gamma_2\int_{-\infty}^{\infty} w\left(0,0,L,y'\right)\xi_2'dy'$$

$$\lambda\xi_2 = -\xi_2 + \Gamma_1\int_{-\infty}^{\infty} w\left(L,0,0,y'\right)\xi_1'dy' + \Gamma_2\int_{-\infty}^{\infty} w\left(0,0,L,y'\right)\xi_2'dy' \qquad (27)$$

where now ξ_i' denotes $\xi_i\left(y'\right)$. Subscripts 1 and 2 designate restrictions to $x = 0$ and $x = L$, respectively, according to $\Gamma_1 = 1/\left|\partial\bar{u}\left(0\right)/\partial x\right|$, $\Gamma_2 = 1/\left|\partial\bar{u}\left(L\right)/\partial x\right|$ and $\xi_1\left(y\right) = \xi\left(0,y\right)$, $\xi_2\left(y\right) = \xi\left(L,y\right)$. Arguing in exactly the same way as when considering annular solutions we conclude that (26) admits an uncountable infinity of eigenvalues which are the same as those of matrices

$$\left[\begin{array}{cc} -1 + \Gamma_1\hat{w}_0\left(\Omega\right) & \Gamma_2\hat{w}_L\left(\Omega\right) \\ \Gamma_1\hat{w}_L\left(\Omega\right) & -1 + \Gamma_2\hat{w}_0\left(\Omega\right) \end{array}\right] \qquad (28)$$

where $\hat{w}_0\left(\Omega\right) = \int_{-\infty}^{\infty} w\left(0,0,0,y'\right)\cos\left(\Omega y'\right)dy' = \int_{-\infty}^{\infty} w\left(L,0,L,y'\right)\cos\left(\Omega y'\right)dy'$, $\hat{w}_L\left(\Omega\right) = \int_{-\infty}^{\infty} w\left(L,0,0,y'\right)\cos\left(\Omega y'\right)dy' = \int_{-\infty}^{\infty} w\left(0,0,L,y'\right)\cos\left(\Omega y'\right)dy'$. To every nonnegative real number corresponds a pair of eigenvalues. The corresponding eigenfunctions can be evaluated from (27).

Acknowledgment

References

S. I. Amari (1977) Dynamics of pattern formation in lateral-inhibition type neural fields. *Biological Cybernetics* **27**, 77-87.

P. Bressloff (2005) Spontaneous symmetry breaking in self-organizing neural fields. *Biological Cybernetics* **93**, 256-274.

M. Camperi, X. J. Wang (1998) A model of visuospatial working memory in prefrontal cortex: Recurrent network and cellular bistability. *Journal of Computational Neuroscience* **5**:4, 383-405.

M. G. Crandall, P. H. Rabinowitz (1971) Bifurcation from simple eigenvalues. *J. Funct. Anal.* **8**, 321-340.

D. W. Dong, J. J. Hopfield (1992) Dynamic properties of neural networks with adapting synapses. *Network: Computation in Neural Systems* **3**:3, 267-283.

K. Doubrovinski (2005) Dynamics, stability and bifurcation phenomena in a nonlocal model of cortical activity.
http://www.matj.uu.se/research/pub/Doubrovinski1.pdf

W. Erlhagen, G. Schöner (2002) Dynamic field theory of movement preparation. *Psychological Review* **109**:3, 545-572.

W. Erlhagen, E. Bicho (2006) The dynamic neural field approach to cognitive robotics. *Journal of Neural Engineering* **3**,R36-R54.

G. B. Ermentrout, J. D. Cowan (1979) A mathematical theory of visual hallucination patterns. *Biological Cybernetics* **34**, 137-150.

G. B. Ermentrout (1998) Neural networks as spatiotemporal pattern forming systems. *Rep. Prog. Phys.* **61**:4, 353-430.

M. A. Giese (1998) *Dynamic neural field theory for motion perception.* Kluwer Academic Publishers, Boston.

H.-M. Gross, V. Stephan, M. Krabbes (1998) A neural field approach to topological reinforcement learning in continuous action spaces. *IEEE World Congress on Comput. Intell.* (1998).

J. M. Herrmann, K. Pawelzik, T. Geisel (1999) Self-localization of autonomous robots by hidden representations. *Autonomous Robots* **7**:1, 31-40.

J. M. Herrmann, H. Schrobsdorff, T. Geisel (2004) Localized activations in a simple neural field model. *CNS 2004.*

I. Iossifidis, A. Steinhage (2001) Controlling an 8 DOF manipulator by means of neural fields. *International Conference on Field and Service Robotics* (2001).

V. K. Jirsa, K. J. Jantzen, A. Fuchs, J. A. S. Kelso (2002) Spatiotemporal forward solution of the EEG and MEG using network modeling. *IEEE Transactions on Medical Imaging* **21**:5, 493-504.

K. Kishimoto, S. I. Amari (1979) Existence and stability of local excitations in homogeneous neural fields. *Mathematical Biology* **7**, 303-318.

E. Kreyszig (1978) *Introductory functional analysis with applications.* Wiley, New York.

C. R. Laing, C. Chow (2001) Stationary bumps in networks of spiking neurons. *Neural Computation* **13**:7, 1473-1494.

C. R. Laing, W. C. Troy, B. S. Gutkin and G. B. Ermentrout (2002) Multiple bumps in a neuronal model of working memory. *SIAM Journal of Applied Mathematics* **63**:1, 62-97.

C. R. Laing, W. C. Troy (2003) PDE methods for nonlocal problems. *SIAM Journal of Dynamical Systems* **2**:3, 487-516.

E. E. Lieke, R. D. Frostig, A. Arieli, D.Y . Ts'o, R. Hildesheim, and A. Grinvald (1989) Optical imaging of cortical activity: Real-time imaging using extrinsic dye-signals and high resolution imaging based on slow intrinsic-signals. *Annu. Rev. Physiol.* **51**, 543-559.

N. Mayer, J. M. Herrmann, T. Geisel (2002) Curved feature metrics in models of visual cortex. *Neurocomputing* **44-46**, 533-539.

L. M. Pismen (1999) *Vortices in nonlinear fields. Form liquid crystals to superfluids. From non-equilibrium patterns to cosmic strings.* Clarendon Press. Oxford Science Publications.

A. Schierwagen, H. Werner (1996) Saccade control through the collicular motor map: Two-dimensional neural field model. In: Lecture Notes In Computer Science. Vol. 1112, Springer-Verlag, 439-444.

A. R. Schutte, J. P. Spencer, G. Schöner (2003) Testing the dynamic field theory: Working memory for locations becomes more spatially precise over development. *Child Development* **74**:5, 1393-1417.

A. Steinhage (2000) The dynamic approach to anthropomorphic robotics. *Proceedings of the fourth Portuguese Conference on Automatic Control, Controlo 2000.*

K. Suder, F. Wörgötter, T. Wennekers (2001) Neural field model of receptive field restructuring in primary visual cortex. *Neural Computation* **13**, 139-159.

A. Takeuchi, S. I. Amari (1979) Formation of topographic maps and columnar microstructures. *Biological Cybernetics* **35**, 63-72.

S. Tanaka, J. Ribot, K. Imamura, T. Tani (2006) Orientation-restricted continuous visual exposure induces marked reorganization of orientation maps in early life. *NeuroImage* **30**:2, 462-477.

J. G. Taylor (1999) Neural 'bubble' dynamics in two dimensions: foundations. *Biological Cybernetics* **80**, 393-409.

E. Thelen, G. Schöner, C. Scheier, L. B. Smith (2001) The dynamics of embodiment: A field theory of infant perseverative reaching. *Behavioral and Brain Sciences* **24**, 1-84.

H. Werner, T. Richter (2001) Circular stationary solutions in two-dimensional neural fields. *Biological Cybernetics* **85**, 211-217.

H. R. Wilson, J. D. Cowan (1973) A mathematical theory of the functional dynamics of cortical and thalamic nervous tissue. *Kybernetik* **13**:2, 55-80.

J. Y. Wu, Y. W. Lam, C. X. Falk, L. B. Cohen, J. Fang, L. Loew, J. Prechtl, D. Kleinfeld, Y. Tsal (1998) Voltage-sensitive dyes for monitoring multineuronal activity in the intact central nervous system. *Histochem. J.* **30**:3, 169-187.